International Journal of Pharmaceutics: X 5 (2023) 100153

Contents lists available at ScienceDirect

International Journal of Pharmaceutics: X

journal homepage: www.sciencedirect.com/journal/international-journal-of-pharmaceutics-x

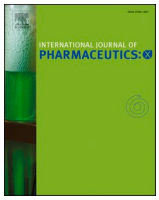

# 3D printed matrix solid forms: Can the drug solubility and dose customisation affect their controlled release behaviour?

Juliana dos Santos [a,f], Gabriela de Souza Balbinot [b], Silvio Buchner [c], Fabrício Mezzomo Collares [b], Maike Windbergs [d], Monique Deon [e,f], Ruy Carlos Ruver Beck [a,f,*]

[a] Programa de Pós-Graduação em Ciências Farmacêuticas, Faculdade de Farmácia Universidade Federal do Rio Grande do Sul, Avenida Ipiranga, 2752, Porto Alegre, Rio Grande do Sul 90610-000, Brazil
[b] Laboratório de Materiais Dentários, Faculdade de Odontologia, Universidade Federal do Rio Grande do Sul, Rua Ramiro Barcelos, 2492/4th floor, Porto Alegre, RS, Brazil
[c] Laboratório de Altas Pressões e Materiais Avançados (LAPMA), Instituto de Física, Universidade Federal do Rio Grande do Sul, Porto Alegre, Rio Grande do Sul, Brazil
[d] Institute of Pharmaceutical Technology and Buchmann Institute for Molecular Life Sciences, Goethe University Frankfurt, Max-von-Laue Straße 9, 60438 Frankfurt am Main, Germany
[e] Programa de Pós-Graduação em Biociências, Universidade Federal de Ciências da Saúde de Porto Alegre, Porto Alegre, RS, Brazil
[f] Laboratório de Nanocarreadores e Impressão 3D em Tecnologia Farmacêutica (Nano3D), Faculdade de Farmácia, Universidade Federal do Rio Grande do Sul (UFRGS), Porto Alegre, Brazil

ARTICLE INFO

*Keywords:*
3D printing
Additive manufacturing
Glucocorticoid
Hot melt extrusion
Implants
Polyester
Printlets

ABSTRACT

The use of 3D printing in pharmaceutics has grown over the last years, along with the number of studies on the impact of the composition of these formulations on their pharmaceutical and biopharmaceutical properties. Recently, we reported the combined effect of the infill percentage and the presence of a pore former on the drug release behaviour of 3D printed matrix solid forms prepared by fused deposition modelling. However, there are some open questions about the effect of the drug solubility and the size of these dosage forms on their controlled release properties. Therefore, we produced poly(Ɛ-caprolactone) filaments containing different soluble forms of dexamethasone (free acid, DEX; acetate ester, DEX-A; and phosphate salt, DEX-P), which showed suitable mechanical properties and printability. 3D printed solid forms were produced in two different sizes. The formulations composed of DEX-P released about 50% of drug after 10 h, while those containing DEX or DEX-A released about 9%. The drug release profiles from the 3D printed forms containing the same drug form but with different sizes were almost completely overlapped. Therefore, these 3D printed matrix solid forms can have their drug content customised by adjusting their size, without changing their controlled release behaviour.

## 1. Introduction

Since 3D printing emerged in the pharmaceutical field, mainly after 2015 when Spritam® came to the market, countless researchers have focused their efforts on discovering the effects of different formulations, excipients and drugs to successfully obtain customised 3D printed dosage forms (Auriemma et al., 2022; Wang et al., 2022). Among the available 3D printing techniques, fused deposition modelling (FDM) is one of the most used in the pharmaceutical area. In this technique, a polymeric filament is extruded at a temperature that will melt it, and it is then deposited layer by layer to form the digitally designed object. FDM has been associated with hot-melt extrusion (HME) for the production of the filaments (Bandari et al., 2021; dos Santos et al., 2021a) and enables the production of pharmaceutical forms with different sizes, geometries and porosities (Goyanes et al., 2015; Sadia et al., 2018).

These formulation modifications are responsible for one of the most important advantages related to 3D printing: the customisation of therapies (Mohammed et al., 2020). The possibility of obtaining drug delivery systems with different sizes and infills impacts their drug content, surface area, surface area/volume ratio and drug release. Depending on this profile, there are different factors that can influence the drug release rate: the properties of the polymer or the blend of polymers, the surface area and surface area/volume ratio of the dosage form (Goyanes et al., 2015), the presence of disintegrants (Funk et al.,

* Corresponding author at: Faculdade de Farmácia, Universidade Federal do Rio Grande do Sul, Av. Ipiranga, 2752, Bairro Santana CEP, 90610-000, Porto Alegre, RS, Brazil.
*E-mail address:* ruy.beck@ufrgs.br (R.C.R. Beck).

https://doi.org/10.1016/j.ijpx.2022.100153
Received 25 November 2022; Received in revised form 21 December 2022; Accepted 22 December 2022
Available online 23 December 2022

2022) or pore formers (dos Santos et al., 2021b), the infill rate (Fanous et al., 2021) and the drug properties (Sadia et al., 2016), among others.

Therefore, the design and development of 3D printed dosage forms with a customised release profile requires a rational rating of the physicochemical characteristics of the drug, including its solubility behaviour, as well as the properties of the polymers, which are key factors in achieving the desired release pattern. The thermal stability of the drug during both hot-melt extrusion and the printing process is also an important parameter to take into account when developing 3D printed forms by a FDM process, as the drug can degrade above a particular temperature, losing its effects or even producing toxic degradation products (Kollamaram et al., 2018).

Dexamethasone (DEX) (Fig. 1A) is a glucocorticoid of synthetic origin derived from cortisol, well-known as a potent anti-inflammatory (Soumya and Joe, 2021) and practically insoluble in water (1 mg $mL^{-1}$) (Drugbank, 2022). It is clinically used as an anti-inflammatory and immunosuppressive agent in the treatment of different chronic diseases, including rheumatoid arthritis, asthma, inflammatory bowel disease (Giron et al., 2019; Mei et al., 2019) and cancer (Pundole and Suarez-Almazor, 2020). It has also been used to prevent some adverse effects in the treatments of cancer (Bashir and Acosta, 2020). More recently, its use in reducing symptoms related to COVID-19 has also been explored (Horby et al., 2020). DEX can be found in the market in the form of a tablet, cream, elixir, injectable solution and ophthalmic suspension, in its free acid (DEX), acetate ester (DEX-A) (Fig. 1B) or sodium phosphate salt (DEX-P) (Fig. 1C). DEX-A is the highest hydrophobic DEX form (water solubility: 0.1 mg $mL^{-1}$), while DEX-P is the highest hydrophilic DEX form (water solubility: 500 mg $mL^{-1}$) (Einmahl et al., 1999). All these DEX forms (DEX, DEX-A and DEX-P) have high melting points and are stable at high temperatures, which make them eligible drugs for the development of 3D printed dosage forms by FDM.

In a previous study, we reported the development of controlled release FDM 3D printed solid forms containing DEX, which was suggested as a suitable platform to design intratumoural implants (dos Santos et al., 2021b). Poly-Ɛ -caprolactone (PCL) was explored as the main polymer due to its non-swellable characteristics and recognised biocompatibility (Ataie et al., 2022; Domínguez-Robles et al., 2021). In that study, we showed that the use of mannitol in the formulation of the solid forms, as a pore former, and changing their infill rate was a promising tool to tailor the drug release rate from the 3D printed forms. However, some questions remain open: how could the solubility of the drug influence the release rate from these 3D printed forms? Would it be possible to customise the drug dose, adjusting their size, without changing the drug release profile?

Therefore, the objective of this study was to evaluate the influence of the drug solubility and the size of the dosage form on the drug release profiles of FDM 3D printed solid forms composed of a biocompatible hydrophobic matrix (PCL). DEX was the drug rationally chosen to answer our questions, since it is available in three different forms (as the free acid form, acetate ester and sodium salt) that have different solubilities (DEX-A < DEX < DEX-P), which helps in understanding the influence of the drug solubility on the release pattern without changing the main skeleton of its chemical structure.

## 2. Material and methods

### 2.1. Material

Dexamethasone, dexamethasone phosphate, mannitol and microcrystalline cellulose (Avicel pH 301) were acquired from Valdequímica (São Paulo, Brazil). Dexamethasone acetate was purchased from Fagron (São Paulo, Brazil). Powder PCL, MW 50,000 Da (Capa™ 6506), was donated by Perstorp (Cheshire, UK). Triethyl citrate (TEC), PEG 6000 and HPLC-grade acetonitrile were purchased from Merck (Darmstadt, Germany). All other chemicals and solvents were of analytical grade and were used as received.

### 2.2. Preparation of drug-loaded filaments

Drug-loaded filaments containing DEX, DEX-A and DEX-P were prepared independently by HME, with the help of a Filmaq 3D extruder (Curitiba, Brazil). The composition of filaments was based on our previous study (dos Santos et al., 2021b), using 5% (*w*/w) DEX, 64% PCL, 10% mannitol, 5% microcrystalline cellulose, 6% TEC and 10% PEG 6000. All components were first mixed with the help of a mortar and pestle for 5 min and were then transferred to the extruder. Filaments containing the different DEX forms were extruded at the same temperature (90 °C) and were prepared with a diameter of 1.75 mm ± 0.05 mm, which was measured, in process, using a digital calliper (Digimess, São Paulo, Brazil).

### 2.3. Mechanical properties of filaments

The tensile strength of the extruded filaments ($n = 6$) was measured using a TA.XT plus Texture Analyser (Stable Micro Systems, Godalming, UK) equipped with a 50 kg load cell and tensile grips (A\TG). Filaments were cut into 50 mm segments and placed vertically in the screw, with a gauge length of 30 mm. Afterwards, each filament was stretched at an elongation speed of 0.8 mm/s until it was broken. Exponent software (Stable Micro Systems, Godalming, UK) was used to record the stress and strain values and to calculate the following parameters: tensile strength, Young's Modulus and elongation at break.

### 2.4. Water contact angle analysis

An optical contact angle (OCA 15LJ, Dataphysics, Filderstadt,

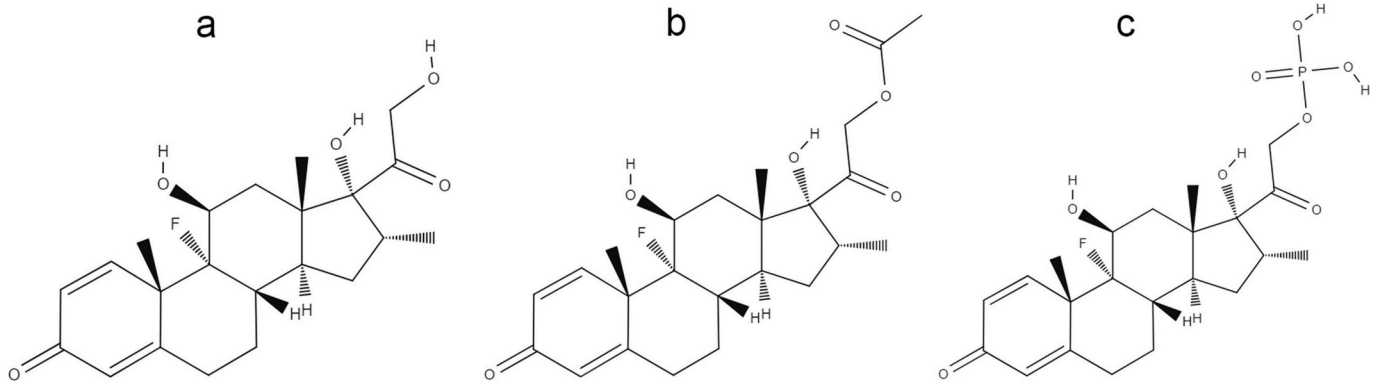


**Fig. 1.** Chemical structure of different dexamethasone forms: (A) dexamethasone free acid (DEX); (B) dexamethasone acetate (DEX-A); and (C) dexamethasone phosphate (DEX-P).

Germany) was used to investigate the surface wettability of the extruded filaments. Filaments were melted at approximately 80 °C and pressed to obtain a thin film. The films obtained from the extruded filaments, films prepared from PCL raw material, and films prepared from a blend of PCL and mannitol were tested ($n = 3$) by applying a 5 μL droplet of deionised water onto their surface. The images of the contact of the drop with the films were recorded and analysed using SCA20 software (V. 5.0.37 build 5037, Dataphysics, Filderstadt, Germany).

### 2.5. Preparation of 3D printed formulations

Solid dosage forms were 3D printed by FDM using the previously extruded filaments (MakerBot Replicator 2× FDM 3D printer, MakerBot Inc., USA) and the following parameters: speed while extruding (90 mm/s), speed while travelling (150 mm/s), number of shells (2), layer thickness (0.20 mm) and an infill rate of 50%. MakerBot Desktop software was used to design the shape of the formulations. They were printed in a cylindrical shape, in two different sizes: (1) 10 mm diameter and 3.6 mm height – named printlets (PRT); and (2) 5 mm diameter and 1.8 mm height – named mini-printlets (MPRT). Therefore, six (6) different formulations were prepared. Table 1 shows the details of the different formulations, as well as their printing temperatures.

### 2.6. Drug content and drug loading

The drug content and drug loading of the filaments, PRT and MPRT were assayed by liquid chromatography (Shimadzu System, Japan) according to a method previously reported (Beber et al., 2016). The assay of the different DEX forms (DEX, DEX-A and DEX-P) was performed using a RP-C18-column (250 × 4.6 mm; 5 μm; Phenomenex Gemini, Torrance, CA, USA). The mobile phase to assay DEX and DEX-A was composed of a mixture of acetonitrile and water (50:50 *v*/v), and the mobile phase to assay DEX-P was composed of a mixture of acetonitrile and phosphate buffer pH 3 (35:65 v/v). Regardless of the DEX form, a flow rate of 1 mL $min^{-1}$ and detection at 240 nm were used. The methods were precise, accurate, and linear in the range of 2.5–50 μg $mL^{-1}$. The drug content was calculated as the amount of drug per tablet (mg/unit), and the drug loading was calculated as the ratio between the amount of drug and the weight of the final solid form (%).

### 2.7. Mean weight, diameter and height

The weight of the solid forms ($n = 10$) was measured with an analytical balance (Shimadzu, Japan) and their mean weight calculated. Their diameter and height (n = 10) were also measured with a digital calliper (Digimess São Paulo, Brazil).

### 2.8. Thermal analysis

All 3D printed solid forms and the PCL, DEX, DEX-A and DEX-P raw materials had their thermal behaviour measured by differential scanning calorimetry (DSC) and thermogravimetric analysis (TGA). DSC analyses were performed using a Shimadzu DSC-60 (Kyoto, Japan). A 5 mg sample was weighed in an aluminium pan. A heating rate of 10 °C $min^{-1}$ was set for the DSC analysis, using nitrogen as the purge gas (50 mL $min^{-1}$). The data were analysed by the Lab Solution TA 60 software (Shimadzu, Kyoto, Japan).

TGA analyses were performed using a thermoanalyser (Shimadzu, TGA-50, Kyoto, Japan), placing the sample in a platinum pan and heating it to 900 °C at a rate of 20 °C $min^{-1}$, with a nitrogen flow of 50 mL $min^{-1}$.

**Table 1**
Printlets (PRT) and mini-printlets (MPRT) prepared with 5% of different dexamethasone forms: dexamethasone free acid (DEX), dexamethasone acetate (DEX-A) and dexamethasone sodium phosphate (DEX-P).

| Formulation | DEX form | Size (d x h, mm) | Printing temperature (°C) |
|---|---|---|---|
| PRT-DEX | DEX | 10 × 3.6 | 105 |
| MPRT-DEX | DEX | 5 × 1.8 | 105 |
| PRT-DEX-A | DEX-A | 10 × 3.6 | 85 |
| MPRT-DEX-A | DEX-A | 5 × 1.8 | 85 |
| PRT-DEX-P | DEX-P | 10 × 3.6 | 110 |
| MPRT-DEX-P | DEX-P | 5 × 1.8 | 110 |

### 2.9. X-ray powder diffraction (XRPD)

All printed solid forms and the PCL, DEX, DEX-A and DEX-P raw materials had their X-ray powder diffraction (XRPD) behaviour analysed by a Rigaku diffractometer (Tokyo Japan), using Cu Kα (λ = 0.154056 nm) as the radiation source, 40 kV voltage, 17 mA current, and a step of 0.05 in the range of 3–60 (2θ).

### 2.10. Raman spectroscopy

Raman measurements of the 3D printed formulations were performed with a 785 nm laser in a Senterra micro-Raman spectrometer (Bruker, Ettlingen, Germany). The whole top surface of each PRT formulation was analysed using a scan area of 25 × 25 measuring points, totalling 625 analysed points. The laser was operated at 100 mW with 5 coadditions per 5 s, with 3–5 $cm^{-1}$ resolution. A Raman spectrum was recorded at each measurement point, and the peak height was used to integrate the results according to the chemical composition of the 3D printed formulation. The DEX (1640 $cm^{-1}$) and mannitol (876 $cm^{-1}$) peaks were quantified (OPUS Spectroscopy Software; Billerica, USA) and used in heat colour mapping, where the high-intensity compounds are shown in orange/red, while low-intensity regions are observed in purple/blue. The reference Raman spectrum of the pure crystalline components was also determined.

### 2.11. In vitro drug release studies

The drug release profiles of the 3D printed solid forms (PRT and MPRT) were evaluated using a USP-I apparatus (model 299 dissolutor, Nova Ética, São Paulo, Brazil). In order to maintain sink conditions and the same proportion of drug/release medium in the release studies, 580 mL or 100 mL of release medium were used for PRT and MPRT, respectively. The study was carried out for 10 h ($n = 3$) and comprised two stages: the dosage forms remained in hydrochloric acid 0.1 mol $L^{-1}$ for 2 h, followed by 8 h in phosphate buffer pH 6.8. At predetermined times, a 5 mL aliquot was collected and replaced with fresh media. The withdrawn samples were filtered and analysed by liquid chromatography, according to the method described in *Section 2.6*. To calculate the mass loss during the experiment (erosion index), the PRT and MPRT were weighed before and after the release study. After removing them from the release basket, the solid forms were carefully dried with tissue paper and maintained in a desiccator until constant weight.

### 2.12. X-ray micro computed tomography

The porosity of the 3D printed dosage forms was assessed by X-ray microtomography (XμCT) (SMX-90 CT; Shimadzu Corp., Kyoto, Japan). Images were taken using 40 kV and 60 mA, with 360° rotation and 1024 × 1024 resolution. Images were reconstructed using the InspeXio SMX-90CT software program (Shimadzu Corp., Kyoto, Japan) and the porosity measurements were carried out with the VGSTUDIOMAX 3.5 software (Volume Graphics GmbH, Heidelberg, Germany) after applying a Gaussian filter and surface determination using a standardised threshold. After segmentation, the percentage of volume occupied by the 3D printed structure and the total volume, including the empty spaces, was calculated. The porosity (%) was calculated based on the percentage of empty volume in the 3D printed formulation.

### 2.13. Statistical analysis

Statistical analysis was carried using Student's *t*-test or one-way ANOVA followed by *post hoc* Tukey's test at a significance level of 5% (GraphPad Prism software, version 5.00.288, GraphPad Software, Inc., USA).

## 3. Results and discussion

### 3.1. Hot-melt extruded filaments

Three different filaments containing different DEX forms were successfully extruded at the same temperature (90 °C), independent of the solubility of the drug form (DEX, DEX-A or DEX-P). They were white and malleable, with a diameter of 1.75 mm ± 0.05 mm. Their drug loadings were close to the designed values: 5.39% ± 0.04% (DEX), 4.92% ± 0.04% (DEX-A) and 5.23% ± 0.10% (DEX-P), showing that there was a good mixture of the components, before and during the extrusion process, as well as demonstrating that no degradation of DEX occurred during the thermal process. This behaviour is in agreement with our previous study reporting the preparation of PCL filaments containing DEX at different drug loading percentages, with or without mannitol (dos Santos et al., 2021b).

However, besides these physicochemical properties, the mechanical properties of the filaments are also decisive in determining whether they are printable or not (Deon et al., 2022). In this sense, we evaluated the mechanical properties of the three different extruded filaments to evaluate whether the DEX form had any impact on them. These data are shown in Table 2. Tensile strength represents the maximum stress that the material supports before breaking and is an important measurement to predict whether the filament could deform or break during handling (Feuerbach et al., 2019). The stiffness of the filament was represented by the Young's Modulus, whereas the elongation at break can give a notion of the flexibility of the material (Prasad et al., 2019). Filaments that are too brittle can break during the feeding process and are considered, in most cases, to be unfeedable or unprintable. Regardless of the parameter evaluated, the solubility of the dexamethasone (DEX form) did not show any effect on the mechanical behaviour of the filaments, which corroborates with the experimental observation, where all filaments had a similar behaviour during the printing process. In addition, these range of values are in agreement with those data reported for filaments composed of ethyl cellulose and different release modifiers, like poly(vinyl alcohol), Soluplus®, PEG 6000, Eudragit® RL PO/RS PO, hydroxypropyl methylcellulose and Kollidon® vinyl acetate 64 (Shi et al., 2021).

### 3.2. 3D printed solid forms

After characterisation of the filaments, the 3D printing of the proposed formulations was performed. Both designed sizes (PRT or MPRT) were successfully printed, regardless of the drug composition (Fig. 2). The solubility of the drug (DEX, DEX-A, DEX-P) did not affect the printability of the filaments, corroborating the data about the mechanical properties of the filaments, as previously discussed. Solid forms containing DEX, DEX-A and DEX-P were printed at a temperature of 105 °C, 85 °C and 110 °C, respectively. A hypothesis for the small differences between the 3D printing temperatures, especially for filaments containing DEX-A, could be the favourable hydrophobic-hydrophobic interactions between the drug and the PCL matrix, affording a better dispersion of the drug in the polymeric matrix.

**Table 2**
Mechanical properties ($n = 6$) of extruded filaments containing different DEX forms: dexamethasone free acid (DEX), dexamethasone acetate (DEX-A) and dexamethasone sodium phosphate (DEX-P). Results are expressed as mean ± SD.

| | Tensile strength (MPa) | Young's Modulus (MPa) | Elongation at break (%) |
|---|---|---|---|
| DEX | 9.10 ± 0.53[a] | 1.19 ± 0.07[a] | 7.35 ± 2.60[a] |
| DEX-A | 10.16 ± 1.09[a] | 1.01 ± 0.12[b] | 9.43 ± 3.04[a] |
| DEX-P | 9.88 ± 1.06[a] | 1.09 ± 0.12[ab] | 8.75 ± 2.06[a] |

Means followed by the same letter, in the same column, are not statistically different (ANOVA, Tukey's test, $p \leq 0.05$).


**Fig. 2.** 3D printed solid forms in two sizes: 10 × 3.6 mm – printlet (PRT); and 5 mm × 1.8 mm – mini-printlet (MPRT).

The physicochemical characteristics of the 3D printed forms are summarised in Table 3. The mean weight was about 0.2 g and 0.03 g for PRT and MPRT, respectively, with low intra-batch variation (USP 41, 2018). The diameter and height values of the MPRT were half of those found for the PRT, which agrees with that previously set by the software. In addition, this result reinforces one of the main features attributed to 3D printing: precision in customisation. Again, the solubility of the different DEX forms had no influence on the physical characteristics of the 3D printed formulations.

However, the solid forms printed with different sizes (PRT and MPRT) made it possible to adjust the drug content per unit, corroborating the feasibility of customising the drug content of pharmaceuticals. The dose customisation of pharmaceutical dosage forms remains one of the main advantages of the 3D printing process. In this sense, PRT were obtained with a drug content of 10 mg/unit, whereas MPRT had a drug

**Table 3**
Physicochemical characteristics of the printlets (PRT) and mini-printlets (MPRT) prepared with different DEX forms: dexamethasone free acid (DEX), dexamethasone acetate (DEX-A) and dexamethasone sodium phosphate (DEX-P). Results are expressed as mean ± SD.

| Formulation | Mean weight (g) | Diameter (mm) | Height (mm) | Drug content (mg/unit) | Drug loading (%) |
|---|---|---|---|---|---|
| PRT-DEX | 0.218 ± 0.014 | 8.96 ± 0.20 | 4.07 ± 0.04 | 10.87 ± 0.26 | 5.40 ± 0.21 |
| MPRT-DEX | 0.035 ± 0.002 | 4.40 ± 0.23 | 2.35 ± 0.04 | 1.90 ± 0.09 | 5.22 ± 0.06 |
| PRT-DEX-A | 0.207 ± 0.011 | 8.60 ± 0.22 | 4.20 ± 0.05 | 9.71 ± 0.35 | 4.87 ± 0.03 |
| MPRT-DEX-A | 0.034 ± 0.002 | 4.28 ± 0.12 | 2.41 ± 0.02 | 1.66 ± 0.14 | 4.96 ± 0.26 |
| PRT-DEX-P | 0.206 ± 0.015 | 8.66 ± 0.21 | 3.99 ± 0.05 | 10.83 ± 0.15 | 5.11 ± 0.26 |
| MPRT-DEX-P | 0.032 ± 0.003 | 4.28 ± 0.13 | 2.29 ± 0.05 | 1.83 ± 0.17 | 5.34 ± 0.10 |

content of about 1.9 mg/unit, regardless of the DEX form. On the other hand, all formulations had similar drug loading (about 5%), independent of the size of the dosage form. These results were in agreement with those previously discussed for the filaments, showing that no degradation occurs during the printing process, which was further investigated by thermal analysis.

Thermal analyses were carried out to evaluate the thermal stability, melting behaviour and crystallinity of DEX in its different forms. The data are shown in Fig. 3. All DEX forms showed thermal stability at the temperature used for the hot-melt extrusion and 3D printing, as shown by the TGA analysis (Fig. 3A, D and G). Around the temperature used in the hot-melt extrusion and 3D printing processes, DEX and DEX-A showed no decrease in the mass, while a slight decrease in the mass in the thermogram of DEX-P was evidenced (Fig. 3G), at around 50 °C, which can be attributed to the loss of water from the sample. The same behaviour was described by Pérez-González et al. (2021) for DEX-P, where a mucoadhesive system were produced with DEX-P and polyvinylpyrrolidone. Furthermore, DSC analysis confirmed the melting point of the three DEX forms, as reported in the literature (DEX: 260 °C; DEX-A: 215 °C; and DEX-P: 220 °C), as well as the melting point of PCL and mannitol (60 °C and 165 °C, respectively) (Fig. 3B, E and H). The exothermic event observed in the melting point range of DEX-P might be related to a possible recrystallization of the drug during the heating process considering that TGA analysis (Fig. 3G) did not show any drug degradation at this temperature. This hypothesis should be further investigated in future studies. Moreover, the DSC thermogram of DEX-P showed an endothermic event below 100 °C indicating a loss of water, corroborating the TGA data. In addition, the TGA and DSC analyses confirmed the thermal stability of all DEX forms at the temperature used in both manufacturing processes (HME and 3D printing), as previously suggested by the data from the drug content assay by HPLC. In addition, the DSC thermograms of the 3D printed forms showed a small endothermic peak for DEX and no endothermic peak in the melting point range of DEX-A and DEX-P, suggesting an amorphisation of the drugs during the printing process.

To confirm the results obtained by DSC, the crystalline pattern of the drugs was further evaluated after the printing process by XRPD analysis. Fig. 3C, F and I show the main peaks attributed to the PCL, DEX, DEX-A and DEX-P (Ajaz et al., 2022; Oshiro et al., 2021), showing that the crystalline pattern of the three DEX forms and PCL remain present, even after thermal processing by hot-melting or 3D printing. In some cases, the heating of the FDM 3D printing process is able to amorphise the drug by its total or partial solubilisation in the polymeric matrix. This event happened when griseofulvin (melting point 220 °C) was used to produce tablets by FDM using hydroxypropyl cellulose as the main polymer at temperatures ranging between 210 °C and 240 °C (Buyukgoz et al., 2021). However, in our study, the printing temperature was set below the melting point of all DEX forms, which could explain why the drug was still present in crystalline form in the printed dosage forms. In addition, the drug solubilisation in the polymeric matrix during the heating process in the DSC analyses can explain the difference between the results found by DSC and XRPD analyses (Dedroog et al., 2020).

In order to evaluate the surface distribution of the raw materials and the drug in the 3D printed dosage forms, Raman microscopy analysis were carried out. As the composition of the filaments and the printing parameters were the same, only the PRT were submitted for this evaluation. Most of the peaks detectable in the Raman spectra of the 3D printed forms were related to PCL, explained by its highest percentage (64%) in their composition. A strong carbonyl stretching mode at around 1721 $cm^{-1}$ was observed for all formulations, denoting the PCL crystalline fraction (Fig. S1). However, the spectra mapping of the DEX forms (DEX, DEX-A, and DEX-P) and mannitol could also be identified on the surface of all PRT formulations (Fig. 4). Raman spectra mappings were constructed based on the peaks related to the chemical spectra of

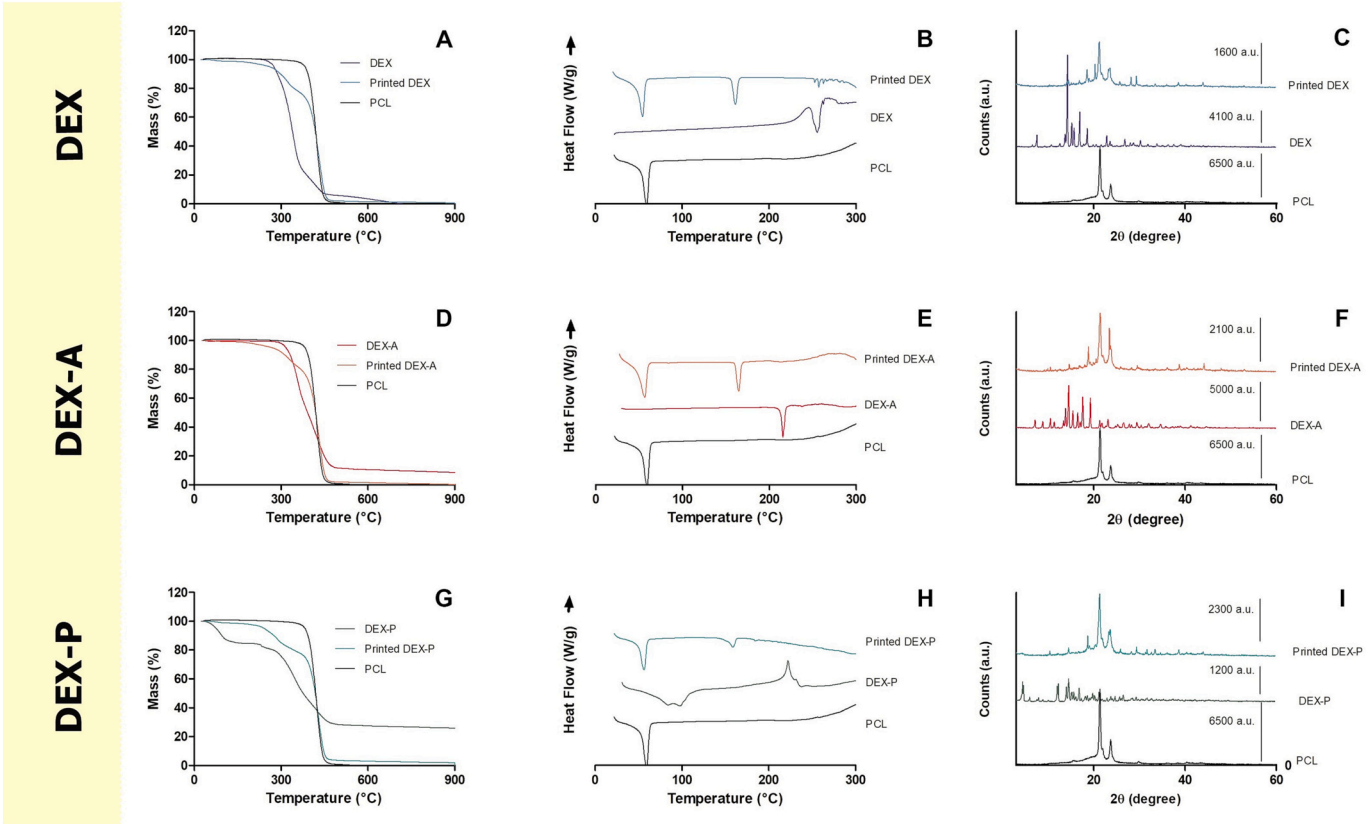


**Fig. 3.** Thermal and X-ray powder diffraction (XRPD) analyses of the 3D printed forms and the PCL, DEX, DEX-A and DEX-P raw materials: thermogravimetric analysis (TGA) thermograms (A, D and G); differential scanning calorimetry (DSC) thermograms (B, E and H); and XRPD) patterns (C, F and I).

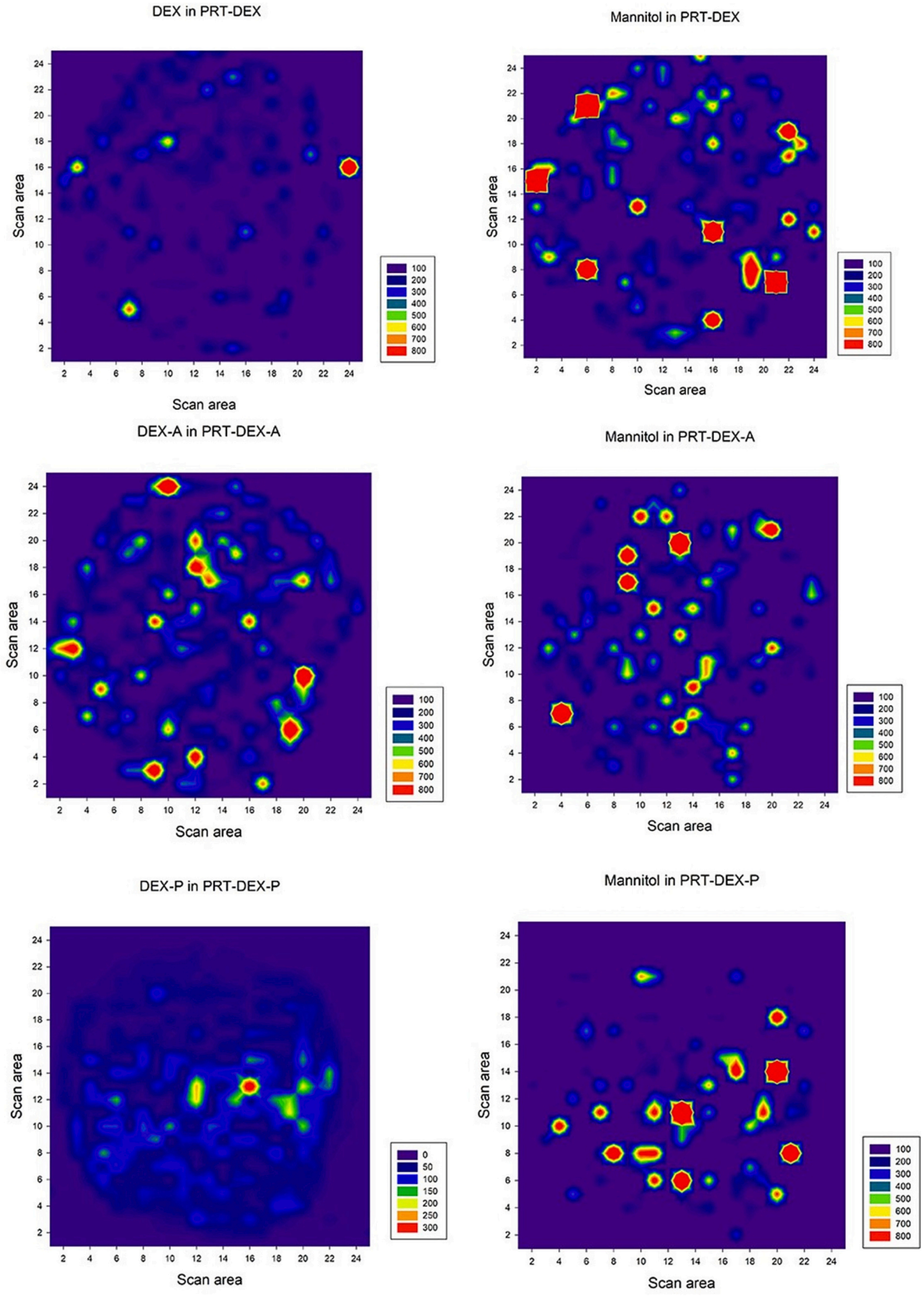


**Fig. 4.** Raman spectra mapping of DEX forms (DEX, DEX-A and DEX-P) and mannitol on the surface of the printlets (PRT).

each component (Fig. S1). DEX has peaks at 1660 $cm^{-1}$ and 1772 $cm^{-1}$ (C═O stretch) (Gupta et al., 2021), which are shared by the three DEX forms. Mannitol was identified by an absorption band at 876 $cm^{-1}$ (Preskar et al., 2021). The shape of this band is sometimes used by some researchers to differentiate between the three polymorphic forms: alpha (α), beta (β) and delta (δ), which can be single, split or slightly shifted, respectively (Burger et al., 2000). Unfortunately, due to the low content of mannitol in the formulations (10%), it was not possible to make this differentiation. However, the conversion of mannitol in polymorphic forms due to the heating process was previously described during the 3D printing of solid forms produced with Eudragit RL (Beck et al., 2017). Regardless of this limitation in discriminating the polymorphic forms of the mannitol, the spectra of the surface of the 3D printed solid forms confirmed the homogeneous incorporation of the drugs in the formulations.

Until now, there has not been any evidence of any significant influence of the solubility of the drug (DEX, DEX-A or DEX-P) on the physicochemical properties of the 3D printed dosage forms, whereas reducing their size enabled the drug content per unit to be decrease. Therefore, the data discussed so far suggest that it is technically possible to adjust the size of the dosage forms to reach a specific drug content. However, considering the development of a controlled release system, adjusting the size of the pharmaceutical form to customise the dose would only be possible if it was not accompanied by a significant change in the drug release profile. Thus, *in vitro* drug release studies were carried out to evaluate the ability of our formulation to keep the same drug release profiles when adjusting the size of the printlets. In addition, the influence of the drug solubility (DEX, DEX-A and DEX-P) on these matrix printlets release profiles was also evaluated. Fig. 5 shows the release profiles of each DEX form from both dosage form sizes (PRT and MPRT). Solid forms containing DEX-P, the most water-soluble DEX form, showed the highest drug release after 10 h (~50%) from both dosage sizes, whereas the forms containing DEX and DEX-A released about 9% of drug from PRT and MPRT during the same period.

Fig. 5 shows almost perfect overlapping of the release profiles from PRT and MPRT, regardless of the DEX form, which is highly important in the context of our study. However, a slightly difference in drug release after 10 h was observed between PRT-DEX and MPRT-DEX. These data mean that the size (and consequently the surface area/volume ratio, whose calculated values were 0.96 $mm^{-1}$ and 1.91 $mm^{-1}$ for PRT and MPRT, respectively) of the solid form did not influence their controlled drug release profiles, regardless of the DEX form. These data are particularly interesting as previous studies have related the influence of the surface area/volume ratio on the drug release from 3D solid forms printed with different sizes and geometries (Goyanes et al., 2015; Windolf et al., 2021), which may affect dose customisation based on tailoring the size of the dosage form. This difference in outcome from our proposed formulation can be explained by the use of an inert polymer as the main printlet matrix. In addition, at the end of our release study experiments, the solid dosage forms remained intact, which allows us to suggest that the main process governing the drug release from these 3D printed forms is drug diffusion, where the medium is able to access the inner structure of the dosage form and drug diffusion occurs *via* channels (Funk et al., 2022). In matrix tablets, it is quite impossible (and challenging) to obtain the same release behaviour for tablets with different sizes, once dissolution starts in these systems without tablet disintegration, and the surface area/volume ratio is a key-factor governing the process (Berardi et al., 2021). However, we were able to produce formulations with different drug doses here, printing them with different sizes, without changing their release rate pattern, thus overcoming an important challenge in the development of matrix tablets. This feature could be attained by preparing PRT and MPRT composed of an inert and biodegradable matrix, using drugs with different solubilities and an infill rate of 50%, which allowed the release medium to access the inner structure of the PRT and MPRT, probably overcoming the effect of the surface area/volume ratio.

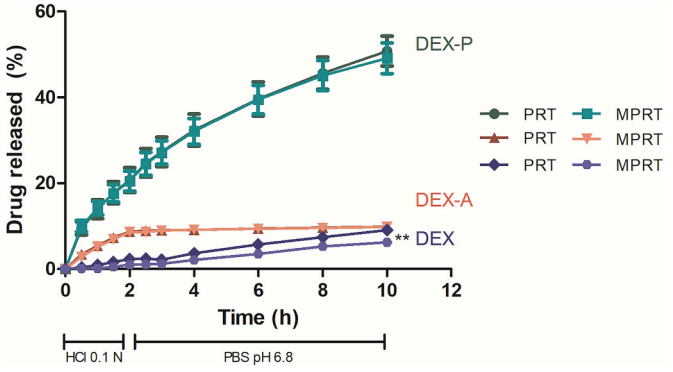


**Fig. 5.** *In vitro* drug release profiles from formulations prepared with different sizes (printlets – PRT and mini-printlets – MPRT) and DEX form (dexamethasone free acid – DEX; dexamethasone acetate – DEX-A; and dexamethasone sodium phosphate – DEX-P). Data are expressed as the mean ± standard deviation and were analysed by two-way ANOVA followed by *post hoc* Bonferroni test. ** significant at $p < 0.01$ for the same DEX form and time.

To evaluate the effect of the erosion processes on the drug release, the erosion index of the formulations was calculated by weighing the solid forms before and after the drug release study. The PRT showed similar erosion indexes: 13.9 ± 1.3%, 12.8 ± 1.6% and 10.3 ± 0.2% for the formulations PRT-DEX-P, PRT-DEX and PRT-DEX-A, respectively ($p > 0.05$). The MPRT also showed similar erosion indexes: 14.1 ± 3.2%, 10.8 ± 1.0% and 11.5 ± 1.0% for MPRT-DEX-P, MPRT-DEX and DEX-A, respectively ($p > 0.05$). A tendency to reach a higher erosion index was observed for the solid forms containing the most water-soluble DEX form (DEX-P), regardless of the dosage size (PRT or MPRT). However, it was not possible to prove a significant mass loss dependent on the DEX form, probably because mannitol, the hydrophilic component present at a higher percentage in these formulations (10% *w*/w), is mainly responsible for the mass loss.

Nevertheless, to further understand the behaviour of the matrix structure of the printlets, their inner structure and their porosity before and after the drug release studies were evaluated by XμCT analysis (Fig. 6). The acquired images of the PRT before the release studies show the layer-by-layer deposition of the material to form the final solid form, and their inner spaces correspond to a 50% infill. These images confirm the accuracy of the printing process, which means that the 3D printed forms match the form designed by the software. On the other hand, the acquired images of the PRT after the release studies do not show evident traces of erosion or increased porosity, as the main structure remained intact, as observed experimentally during the release studies and corroborating the calculated erosion index, as discussed above.

However, Table 4 shows the porosity data calculated from the XμCT images of the PRT before and after the release studies, where the same differences can be observed. Printlets containing DEX-P showed a clear increase in their porosity (~ 18%), whereas those prepared with the other DEX forms only showed a slight tendency to increase. This result agrees with the drug release data, which showed a higher drug release from the 3D printed solid forms containing DEX-P (the most hydrophilic DEX form used in this study). This finding reinforces our hypothesis about the entrance of the release medium into the inner structure of the 50% filled dosage forms, followed by drug diffusion as the main processes governing the release from the PRT and MPRT composed of PCL.

In our previous study, we explained the main effect of mannitol on the drug release rate from PCL 3D printed solid forms as a pore former (dos Santos et al., 2021b). However, the porosity data obtained in this present study do not support this previous hypothesis, probably because of the high hydrophobic property of the main polymeric material (PCL) and the low percentage of mannitol in the formulation (10% *w*/w). Therefore, we raise here the hypothesis that mannitol could also be acting by changing the hydrophobic properties of the printlet matrix.

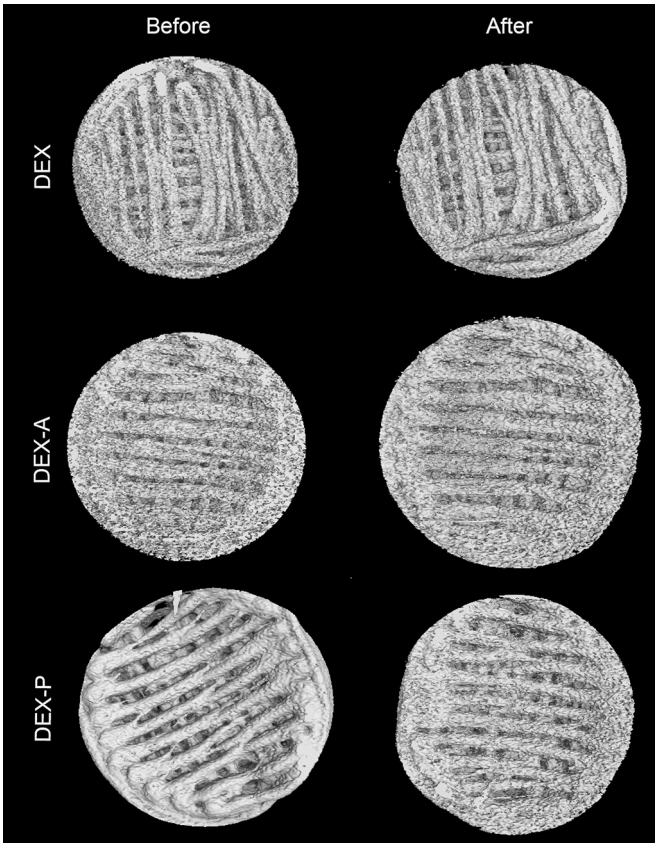


**Fig. 6.** Visualisation of X-ray micro computed tomography (XμCT) data for the top view of PRT before and after the dissolution studies.

**Table 4**
Porosity of the printlets (PRT) prepared with different DEX forms. Porosity was calculated from the XμCT images before and after the drug release studies.

| | Porosity (%) | |
|---|---|---|
| | Before | After |
| PRT-DEX | 57.63 | 58.53 |
| PRT-DEX-A | 59.62 | 62.02 |
| PRT-DEX-P | 41.26 | 59.73 |

This hypothesis was tested by evaluating the wettability of the 3D printed formulations. The wettability of a formulation is closely related to its hydrophobicity (Fan et al., 2021) and can impact the drug release. As a general rule, systems can be classified as hydrophilic when the measured contact angle is $<90°$, or hydrophobic when the contact angle is $>90°$ (Simpson et al., 2015). Our formulations had contact angles between 50° and 90°, with slight variations depending on the solubility of the DEX form (DEX formulation: 69.6°; DEX-A formulation: 58.7°; and DEX-P formulation: 69.2°) (Fig. S2). From these data, they can be considered partially wettable, and the DEX solubility had no influence on their wettability, probably because the amount of drug (5% w/w) was not able to affect the water surface contact. However, the wettability analysis of films prepared with PCL only or with a blend or PCL and mannitol (1:10 w/w) afforded a surface contact angle of 92.2° (not wettable) and 72.4° (partially wettable), respectively. These data reflect a significant influence of mannitol on the wettability of the PCL matrix, and therefore confirm its ability to improve the PCL wettability, as hypothesised above. The correlation between the addition of a component that has affinity with water and the improvement of wettability was previously described when increased amounts of polyethylene glycol (4, 6 and 8% w/w) were added to DEX-polylactic acid scaffolds (Li et al., 2018).

In summary, our data showed that the presence of mannitol can improve the release rate of 3D printed solid forms, as a wetting agent along with its action as a pore former. In this sense, we are designing future studies to evaluate the use of a polymeric blend of PCL and a less hydrophobic polymer as an approach to increase the *in vitro* drug release rate in the first 10 h, which would fit better to the optimal release pattern from an oral dosage form.

## 4. Conclusion

In this study, we have shown the ability to customise the drug dose by FDM 3D printing using a hydrophobic matrix composed of PCL, as the biocompatible polymer. The versatility of the proposed formulation was supported by using active pharmaceutical ingredients with different aqueous solubilities (DEX-P > DEX > DEX-A). The solubility of the dexamethasone form had an important effect on the drug release rate, where the dosage forms produced with the phosphate sodium salt, which is the most hydrophilic form, afforded a faster release than those containing its free acid or acetate ester form. Moreover, beyond providing dose customisation, adjusting the size of the printed solid form (and consequently the surface area/volume ratio) did not change the controlled drug release pattern, indicating an interesting horizon for the production of 3D printed matrix solid forms with customisable drug content, which cannot generally be achieved by traditional methods of tablets production. Expanding the range of this proof-of-concept study, the approach proposed here can be applied in the development of solid dosage forms such as oral printlets and implants.

## Declaration of Competing Interest

The authors report no conflict of interest.

## Data availability

Data will be made available on request.

## Acknowledgements

This work was supported by CNPq/Brazil, CAPES/Brazil (Finance Code 001) and FAPERGS/Brazil. J. dos Santos thanks CAPES and DAAD for her PhD fellowships.

## Appendix A. Supplementary data

Supplementary data to this article can be found online at https://doi.org/10.1016/j.ijpx.2022.100153.

## References

Ajaz, N., Khan, I.U., Irfan, M., Khalid, S.H., Asghar, S., Mehmood, Y., Asif, M., Usra, Hussain, Shahzad, Y., Shah, S.U., Munir, M.U., 2022. In vitro and biological characterization of dexamethasone sodium phosphate laden pH-sensitive and mucoadhesive hydroxy propyl β-cyclodextrin-g-poly(Acrylic Acid)/gelatin semi-interpenetrating networks. Gels 8. https://doi.org/10.3390/gels8050290.

Ataie, M., Nourmohammadi, J., Seyedjafari, E., 2022. Carboxymethyl carrageenan immobilized on 3D-printed polycaprolactone scaffold for the adsorption of calcium phosphate/strontium phosphate adapted to bone regeneration. Int. J. Biol. Macromol. 206, 861–874. https://doi.org/10.1016/j.ijbiomac.2022.03.096.

Auriemma, G., Tommasino, C., Falcone, G., Esposito, T., Sardo, C., Aquino, R.P., 2022. Additive manufacturing strategies for personalized drug delivery systems and medical devices: fused filament fabrication and semi solid extrusion. Molecules 27. https://doi.org/10.3390/molecules27092784.

Bandari, S., Nyavanandi, D., Dumpa, N., Repka, M.A., 2021. Coupling hot melt extrusion and fused deposition modeling: critical properties for successful performance. Adv. Drug Deliv. Rev. 172, 52–63. https://doi.org/10.1016/j.addr.2021.02.006.

Bashir, Q., Acosta, M., 2020. Comparative safety, bioavailability, and pharmacokinetics of oral dexamethasone, 4-mg and 20-mg Tablets, in healthy volunteers under fasting and fed conditions: a randomized open-label, 3-way crossover study. Clin. Lymphoma Myeloma Leuk. 20, 768–773. https://doi.org/10.1016/j.clml.2020.06.022.

Beber, T.C., de Andrade, D.F., dos Santos Chaves, P., Pohlmann, A.R., Guterres, S.S., Ruver Beck, R.C., 2016. Cationic polymeric nanocapsules as a strategy to target dexamethasone to viable epidermis: skin penetration and permeation studies. J. Nanosci. Nanotechnol. 16, 1331–1338. https://doi.org/10.1166/jnn.2016.11670.

Beck, R.C.R., Chaves, P.S., Goyanes, A., Vukosavljevic, B., Buanz, A., Windbergs, M., Basit, A.W., Gaisford, S., 2017. 3D printed tablets loaded with polymeric nanocapsules: an innovative approach to produce customized drug delivery systems. Int. J. Pharm. 528, 268–279. https://doi.org/10.1016/j.ijpharm.2017.05.074.

Berardi, A., Bisharat, L., Quodbach, J., Abdel Rahim, S., Perinelli, D.R., Cespi, M., 2021. Advancing the understanding of the tablet disintegration phenomenon – an update on recent studies. Int. J. Pharm. 598, 120390 https://doi.org/10.1016/j.ijpharm.2021.120390.

Burger, A., Henck, J.O., Hetz, S., Rollinger, J.M., Weissnicht, A.A., Stöttner, H., 2000. Energy/temperature diagram and compression behavior of the polymorphs of D-mannitol. J. Pharm. Sci. 89, 457–468. https://doi.org/10.1002/(SICI)1520-6017(200004)89:4<457::AID-JPS3>3.0.CO;2-G.

Buyukgoz, G.G., Kossor, C.G., Davé, R.N., 2021. Enhanced supersaturation via fusion-assisted amorphization during fdm 3d printing of crystalline poorly soluble drug loaded filaments. Pharmaceutics 13, 28–33. https://doi.org/10.3390/pharmaceutics13111857.

Dedroog, S., Pas, T., Vergauwen, B., Huygens, C., Van den Mooter, G., 2020. Solid-state analysis of amorphous solid dispersions: why DSC and XRPD may not be regarded as stand-alone techniques. J. Pharm. Biomed. Anal. 178, 112937 https://doi.org/10.1016/j.jpba.2019.112937.

Deon, M., dos Santos, J., de Andrade, D.F., Beck, R.C.R., 2022. A critical review of traditional and advanced characterisation tools to drive formulators towards the rational development of 3D printed oral dosage forms. Int. J. Pharm. 628, 122293 https://doi.org/10.1016/j.ijpharm.2022.122293.

Domínguez-Robles, J., Shen, T., Cornelius, V.A., Corduas, F., Mancuso, E., Donnelly, R.F., Margariti, A., Lamprou, D.A., Larrañeta, E., 2021. Development of drug loaded cardiovascular prosthesis for thrombosis prevention using 3D printing. Mater. Sci. Eng. C 129. https://doi.org/10.1016/j.msec.2021.112375.

dos Santos, J., Silveira, G., Velho, M.C., Carlos, R., Beck, R., 2021a. Eudragit® : a Versatile Family of Polymers for Hot Melt Extrusion and 3D Printing Processes in Pharmaceutics. Pharmaceuticals 13, 1424. https://doi.org/10.3390/pharmaceutics13091424.

dos Santos, J., Deon, M., da Silva, G.S., Beck, R.C.R., 2021b. Multiple variable effects in the customisation of fused deposition modelling 3D-printed medicines: a design of experiments (DoE) approach. Int. J. Pharm. 597, 120331 https://doi.org/10.1016/j.ijpharm.2021.120331.

Drugbank, 2022. Dexamethasone - DrugBank. [online]. Available at: https://go.drugbank.com/drugs/DB01234> [Accessed October 2022].

Einmahl, S., Zignani, M., Varesio, E., Heller, J., Veuthey, J.L., Tabatabay, C., Gurny, R., 1999. Concomitant and controlled release of dexamethasone and 5-fluorouracil from poly(ortho ester). Int. J. Pharm. 185 (2), 189–198. https://doi.org/10.1016/S0378-5173(99)00149-0.

Fan, R., Chuan, D., Hou, H., Chen, H., Xu, J., Guo, G., 2021. Development and evaluation of a novel biodegradable implants with excellent inflammatory response suppression effect by hot-melt extrusion. Eur. J. Pharm. Sci. 166, 105981 https://doi.org/10.1016/j.ejps.2021.105981.

Fanous, M., Bitar, M., Gold, S., Sobczuk, A., Hirsch, S., Ogorka, J., Imanidis, G., 2021. Development of immediate release 3D-printed dosage forms for a poorly water-soluble drug by fused deposition modeling: Study of morphology, solid state and dissolution. Int. J. Pharm. 599, 120417 https://doi.org/10.1016/j.ijpharm.2021.120417.

Feuerbach, T., Callau-Mendoza, S., Thommes, M., 2019. Development of filaments for fused deposition modeling 3D printing with medical grade poly(lactic-co-glycolic acid) copolymers. Pharm. Dev. Technol. 24, 487–493. https://doi.org/10.1080/10837450.2018.1514522.

Funk, N.L., Fantaus, S., Beck, R.C.R., 2022. Immediate release 3D printed oral dosage forms: how different polymers have been explored to reach suitable drug release behaviour. Int. J. Pharm. 625, 122066 https://doi.org/10.1016/j.ijpharm.2022.122066.

Giron, F., Pastó, A., Tasciotti, E., Abraham, B.P., 2019. Nanotechnology in the treatment of inflammatory bowel disease. Inflamm. Bowel Dis. 25, 1871–1880. https://doi.org/10.1093/ibd/izz205.

Goyanes, A., Robles, P., Buanz, A., Basit, A.W., Gaisford, S., 2015. Effect of geometry on drug release from 3D printed tablets. Int. J. Pharm. 494, 657–663. https://doi.org/10.1016/j.ijpharm.2015.04.069.

Gupta, Nilkantha, Kamath, S., Rao, S.K., Jaison, D., Patil, S., Neha, Gupta, Arunachalam, K.D., 2021. Kaempferol loaded albumin nanoparticles and dexamethasone encapsulation into electrospun polycaprolactone fibrous mat – concurrent release for cartilage regeneration. J. Drug Deliv. Sci. Technol. 64, 102666 https://doi.org/10.1016/j.jddst.2021.102666.

Horby, P., Lim, W.S., Emberson, J.R., Mafham, M., Bell, J.L., Linsen, L., Staplin, N., Brightling, C., Ustianowski, A., 2020. Dexamethasone in Hospitalized patients with Covid-19 — preliminary Report. N. Engl. J. Med. 1–11 https://doi.org/10.1056/nejmoa2021436.

Kollamaram, G., Croker, D.M., Walker, G.M., Goyanes, A., Basit, A.W., Gaisford, S., 2018. Low temperature fused deposition modeling (FDM) 3D printing of thermolabile drugs. Int. J. Pharm. 545, 144–152. https://doi.org/10.1016/j.ijpharm.2018.04.055.

Li, X., Wang, Y., Wang, Z., Qi, Y., Li, L., Zhang, P., Chen, X., 2018. Composite PLA / PEG / nHA / Dexamethasone Scaffold prepared by 3D Printing for Bone Regeneration. Macromol. Biosci. 18, 1–11. https://doi.org/10.1002/mabi.201800068.

Mei, D., Tan, W.S.D., Wong, W.S.F., 2019. Pharmacological strategies to regain steroid sensitivity in severe asthma and COPD. Curr. Opin. Pharmacol. 46, 73–81. https://doi.org/10.1016/j.coph.2019.04.010.

Mohammed, A., Elshaer, A., Sareh, P., Elsayed, M., Hassanin, H., 2020. Additive manufacturing technologies for drug delivery applications. Int. J. Pharm. 580, 119245 https://doi.org/10.1016/j.ijpharm.2020.119245.

Oshiro, J.A., Lusuardi, A., Beamud, E.M., Chiavacci, L.A., Cuberes, M.T., 2021. Nanostructural arrangements and surface morphology on ureasil-polyether films loaded with dexamethasone acetate. Nanomaterials 11, 1–19. https://doi.org/10.3390/nano11061362.

Pérez-González, G.L., Villarreal-Gómez, L.J., Olivas-Sarabia, A., Valdez, R., Cornejo-Bravo, J.M., 2021. Development, characterization, and in vitro assessment of multilayer mucoadhesive system containing dexamethasone sodium phosphate. Int. J. Polym. Mater. Polym. Biomater. 70, 1316–1328. https://doi.org/10.1080/00914037.2020.1798433.

Prasad, E., Islam, M.T., Goodwin, D.J., Megarry, A.J., Halbert, G.W., Florence, A.J., Robertson, J., 2019. Development of a hot-melt extrusion (HME) process to produce drug loaded AffinisolTM 15LV filaments for fused filament fabrication (FFF) 3D printing. Addit. Manuf. 29, 100776 https://doi.org/10.1016/j.addma.2019.06.027.

Preskar, M., Korasa, K., Vrbanec, T., Klement, D., Vrečer, F., Gašperlin, M., 2021. Applicability of Raman and near-infrared spectroscopy in the monitoring of freeze-drying injectable ibuprofen. Drug Dev. Ind. Pharm. 47, 758–769. https://doi.org/10.1080/03639045.2021.1934864.

Pundole, X., Suarez-Almazor, M.E., 2020. Cancer and Rheumatoid Arthritis. Rheum. Dis. Clin. N. Am. 46, 445–462. https://doi.org/10.1016/j.rdc.2020.05.003.

Sadia, M., Sośnicka, A., Arafat, B., Isreb, A., Ahmed, W., Kelarakis, A., Alhnan, M.A., 2016. Adaptation of pharmaceutical excipients to FDM 3D printing for the fabrication of patient-tailored immediate release tablets. Int. J. Pharm. 513, 659–668. https://doi.org/10.1016/j.ijpharm.2016.09.050.

Sadia, M., Arafat, B., Ahmed, W., Forbes, R.T., Alhnan, M.A., 2018. Channelled tablets : an innovative approach to accelerating drug release from 3D printed tablets. J. Control. Release 269, 355–363. https://doi.org/10.1016/j.jconrel.2017.11.022.

Shi, K., Slavage, J.P., Maniruzzaman, M., Nokhodchi, A., 2021. Role of release modifiers to modulate drug release from fused deposition modelling (FDM) 3D printed tablets. Int. J. Pharm. 597, 120315 https://doi.org/10.1016/j.ijpharm.2021.120315.

Simpson, J.T., Hunter, S.R., Aytug, T., 2015. Superhydrophobic materials and coatings: a review. Rep. Prog. Phys. 78 https://doi.org/10.1088/0034-4885/78/8/086501.

Soumya, S., Joe, I.H., 2021. A combined experimental and quantum chemical study on molecular structure, spectroscopic properties and biological activity of anti-inflammatory Glucocorticosteroid drug. Dexamethasone. J. Mol. Struct. 1245, 130999 https://doi.org/10.1016/j.molstruc.2021.130999.

USP 41, 2018. The United States Pharmacopoeia. Rockville.

Wang, N., Shi, H., Yang, S., 2022. 3D printed oral solid dosage form: Modified release and improved solubility. J. Control. Release 351, 407–431. https://doi.org/10.1016/j.jconrel.2022.09.023.

Windolf, H., Chamberlain, R., Quodbach, J., 2021. Predicting drug release from 3D printed oral medicines based on the surface area to volume ratio of tablet geometry. Pharmaceutics 13. https://doi.org/10.3390/pharmaceutics13091453.